Calculation of the transport and relaxation properties of methane. I. Shear viscosity, viscomagnetic effects, and self-diffusion

Robert Hellmann,[1] Eckard Bich,[1] Eckhard Vogel,[1] Alan S. Dickinson,[2,a)] and Velisa Vesovic[3]
[1]*Institut für Chemie, Universität Rostock, D-18059 Rostock, Germany*
[2]*School of Natural Sciences (Physics), Newcastle University, Newcastle upon Tyne NE1 7RU, United Kingdom*
[3]*Department of Earth Science and Engineering, Imperial College London, London SW7 2AZ, United Kingdom*

(Received 16 June 2008; accepted 24 June 2008; published online 11 August 2008)

Transport properties of pure methane gas have been calculated in the rigid-rotor approximation using the recently proposed intermolecular potential energy hypersurface [R. Hellmann *et al.*, J. Chem. Phys. **128**, 214303 (2008)] and the classical-trajectory method. Results are reported in the dilute-gas limit for shear viscosity, viscomagnetic coefficients, and self-diffusion in the temperature range of 80–1500 K. Compared with the best measurements, the calculated viscosity values are about 0.5% too high at room temperature, although the temperature dependence of the calculated values is in very good agreement with experiment between 210 and 390 K. For the shear viscosity, the calculations indicate that the corrections in the second-order approximation and those due to the angular-momentum polarization are small, less than 0.7%, in the temperature range considered. The very good agreement of the calculated values with the experimental viscosity data suggests that the rigid-rotor approximation should be very reasonable for the three properties considered. In general, the agreement for the other measured properties is within the experimental error. © *2008 American Institute of Physics*. [DOI: 10.1063/1.2958279]

I. INTRODUCTION

The transport properties of gases are a direct consequence of molecular motion and the resulting exchange of angular momentum and energy between colliding molecules. For dilute systems, where only binary interactions are significant, transport properties can be related by means of formal kinetic theory[1] to generalized cross sections. These cross sections are determined by the dynamics of the binary collisions in the gas and can, in turn, be related to the intermolecular potential energy hypersurface that describes a particular molecular interaction.

It is now possible to calculate accurately the generalized cross sections, and hence the transport and relaxation properties, of simple molecular gases directly from the intermolecular potential, both for atom-diatom systems[2] and molecule-molecule systems.[3–9] The accuracy of such calculations is generally commensurate with the best available experimental data and their usefulness self-evident. These calculations provide a stringent test of the accuracy of the potential surface[2–9] and improve our insight into the dominant microscopic processes determining macroscopic transport and relaxation properties. Furthermore, at low and high temperatures where experimental data are of lower accuracy or nonexistent, the calculations can and do provide a better way of estimating transport properties.

In principle, one should perform calculations of transport and relaxation properties from the intermolecular potential by employing a quantum-mechanical formalism. This is at present not computationally feasible for molecule-molecule systems, except possibly for pure hydrogen at low temperatures, and instead a classical description is used. The method of choice is a classical-trajectory calculation which is nowadays computationally fast and, more importantly, accurate, at the temperatures of interest to this work. The accuracy has been attested by a detailed comparison with the quantum calculations for the $He-N_2$ system,[10,11] and the recent success in reproducing highly accurate viscosity measurements near room temperature in carbon dioxide[7] is very encouraging.

The work presented in this paper is a continuation of our previous study[7–9] and aims to improve our knowledge of the transport and relaxation properties of methane. Methane is relevant in a particularly wide variety of both scientific and engineering contexts: it is a feedstock for artificial diamond production; it is a significant greenhouse gas whose effects must be included in climate modeling; it is of importance in planetary studies as it occurs in Titan's atmosphere; being the main constituent of natural gas, it is a critical part of the current and future energy mix; methane is stored in permafrost hydrates, a plausible future energy source. Although transport property data for methane are available, see Sec. IV below, they cluster and are of acceptable accuracy only around room temperature.

In the present paper, we report on calculations of the shear viscosity, viscomagnetic effects, and the self-diffusion coefficient of methane in the temperature range of 80–1500 K. The relevant generalized cross sections have

a)Electronic mail: a.s.dickinson@ncl.ac.uk.

been evaluated by means of the classical-trajectory calculations directly from the available intermolecular potential surface for the methane-methane interaction. For linear molecules, the working expressions for the generalized cross sections in terms of properties of individual trajectories were derived by Curtiss.[12] The extension to asymmetric tops (and hence spherical tops such as methane) has been provided.[13]

For these calculations, we have employed a recent *ab initio* potential[14] that has been adjusted to and validated against accurate experimental second pressure virial coefficient data. The calculations were performed on the assumption that both methane molecules behave as rigid rotors. This assumption was dictated by the nature of the available intermolecular potential, which was developed using the zero-point vibrationally averaged configuration.

For the transport properties of interest, here it has been shown that, at least for carbon dioxide,[7] the effects of the neglect of vibrational motion are small. For methane, the lowest vibrational frequency (1306 cm^{-1}) is much higher than that in carbon dioxide (667.3 cm^{-1}). Inelastic collisions resulting in exchange of vibrational energy are rare, and it is not expected that the vibrational state of the molecule would significantly influence the transport of momentum and mass in a fluid. Nevertheless, the approximate procedure for the inclusion of the effects of the vibrational degrees of freedom, described in our previous work,[6–9] has been implemented to correct, where necessary, the generalized cross sections.

The availability of these classical-trajectory results allows for the first assessment of the accuracy of approximations for the collisions of spherical-top molecules. In particular, the widely used Mason–Monchick[15,16] approximation (MMA), with quantal analog the infinite-order sudden[17] approximation, is investigated along with the use of simply the spherical component of the molecule-molecule potential surface.

II. THEORY

A. Field-free properties

The shear viscosity η and self-diffusion coefficient D of a polyatomic gas at zero density and in the absence of external fields can be expressed as[1,18]

$$\eta = \frac{k_B T}{\langle v \rangle_0} \frac{f_\eta^{(n)}}{\mathfrak{S}(2000)}, \tag{1}$$

$$D = \frac{k_B T}{nm\langle v \rangle_0} \frac{f_D^{(n)}}{\mathfrak{S}'(1000)}, \tag{2}$$

where $\langle v \rangle_0 = 4(k_B T/\pi m)^{1/2}$ is the average relative thermal speed, n is the number density, m is the molecular mass, T is the temperature, and k_B is Boltzmann's constant.

The customary notation[1] $\bar{\mathfrak{S}}\left(\begin{smallmatrix} p & q & s & t \\ p' & q' & s' & t' \end{smallmatrix}\right)_\kappa$ is employed in labeling the generalized cross sections, which include details of the dynamics of the binary encounters in the pure gas, with appropriate statistical averaging over the internal states and translational energy. Thus, the indices p, p' and q, q' denote tensorial ranks in the reduced relative velocity $\mathbf{W}$ and in the rotational angular momentum $\mathbf{j}$, respectively. *Barred* cross sections, as calculated here,[19,20] are defined using the tensor rank κ given by $\boldsymbol{\kappa} = \mathbf{p} + \mathbf{q} = \mathbf{p}' + \mathbf{q}'$. An alternative coupling, $\boldsymbol{\kappa} = \mathbf{p} + \mathbf{p}' = \mathbf{q} + \mathbf{q}'$, yields what are often described[1,21] as *unbarred* cross sections. As differences from the unbarred cross sections arise only when both p and q or both p' and q' are nonzero, we do not indicate the bar unless the barred and unbarred cross sections differ. Relations between the barred and unbarred cross sections can be obtained in Refs. 1 and 21. For notational convenience, when $p'q's't' = pqst$ just one row is retained. If the value of κ is unique, it is omitted. Diagonal and off-diagonal cross sections are referred to as transport [those $\mathfrak{S}(pqst)$ with $p \neq 0$] or relaxation [those $\mathfrak{S}(pqst)$ with $p = 0$] and production or coupling cross sections, respectively. The quantities $\mathfrak{S}(2000)$ and $\mathfrak{S}'(1000)$ are the generalized viscosity and self-diffusion cross sections, respectively (see Ref. 7 for a discussion of the primed diffusion cross section in a pure gas).

The quantities $f_\eta^{(n)}$ and $f_D^{(n)}$ are nth-order correction factors and account for the effects of higher basis-function terms in the perturbation-series expansion of the solution of the Boltzmann equation.[1] In this work, we consider the second- and third-order approximations for viscosity only since for polyatomics no higher-order expressions for diffusion have been developed, although an estimate is available, based on the correction for spherical systems (see Sec. IV D 1). All the available analyses of calculations for monatomic[22,23] and polyatomic[3–9] species indicate that contributions of higher-order approximations for shear viscosity are, at most, $\pm(1-2)\%$.

For polyatomic molecules, the tensorial basis functions describing both velocity coupling[1,24] and angular-momentum coupling[1,25,26] should be included in the higher-order expansion. Traditionally,[1] these polarizations were treated separately, giving rise to separate expressions for the higher-order correction factors. Here, however, following Ref. 4, we have used a single expansion describing both couplings. In the second-order expansion for viscosity, one needs to include, apart from the first-order basis function Φ^{2000}, also basis functions Φ^{2010} and Φ^{2001}, corresponding to velocity coupling[7] (note that contrary to Ref. 27, the basis function Φ^{2011} has not been considered here) and the basis function Φ^{0200}, allowing for angular-momentum coupling.[25]

The higher-order viscosity correction factor is given, in general, as

$$f_\eta^{(n)} = \mathfrak{S}(2000)\frac{S_{11}^{(n)}}{S^{(n)}}, \tag{3}$$

with $S^{(n)}$ as the determinant of cross sections generated by the chosen basis and $S_{11}^{(n)}$ its minor. For $S^{(2)}$, we have

$$S^{(2)} = \begin{vmatrix} \mathfrak{S}(2000) & \mathfrak{S}\binom{2000}{2010} & \mathfrak{S}\binom{2000}{2001} & \mathfrak{S}\binom{2000}{0200} \\ \mathfrak{S}\binom{2010}{2000} & \mathfrak{S}(2010) & \mathfrak{S}\binom{2010}{2001} & \mathfrak{S}\binom{2010}{0200} \\ \mathfrak{S}\binom{2001}{2000} & \mathfrak{S}\binom{2001}{2010} & \mathfrak{S}(2001) & \mathfrak{S}\binom{2001}{0200} \\ \mathfrak{S}\binom{0200}{2000} & \mathfrak{S}\binom{0200}{2010} & \mathfrak{S}\binom{0200}{2001} & \mathfrak{S}(0200) \end{vmatrix}. \tag{4}$$

To calculate the second-order viscosity correction factor $f_\eta^{(2)}$ [Eq. (3)], we need knowledge of three transport cross sections, one relaxation cross section, and six production cross sections. In order to assess the relative importance of the velocity and the angular-momentum coupling, we introduce $f_\eta^{(2')}$, where only the two velocity couplings are included[7] and $S^{(2')}$ is a 3×3 determinant.

To include the velocity coupling up to third order, with third-order correction $f_\eta^{(3)}$, one needs to add three further basis functions, namely, Φ^{2020}, Φ^{2011}, and Φ^{2002}, which result in a 7×7 determinant $S^{(3)}$ similar in structure to $S^{(2)}$.

It is also of interest to examine the relation between the diffusion coefficient and the viscosity as a function of temperature. It is customary in kinetic theory to do this by defining the dimensionless parameter A^* as[22,24]

$$A^* = \frac{5}{6}\frac{\mathfrak{S}(2000)}{\mathfrak{S}'(1000)}. \tag{5}$$

The studies carried out so far on monatomic[22] and polyatomic species[7,28] indicate that the value of this parameter is nearly independent of the potential surface and only weakly dependent on the reduced temperature. These properties have led traditionally to the use of the value of A^* to infer the values of binary diffusion coefficients from measurements of the viscosity of mixtures.[22]

B. Field effects

The viscosity and diffusion coefficients of polyatomic molecules are influenced by the presence of magnetic and electrical fields. Although the effect of an external field is small,[1] it has been measured for a variety of molecules[29] and it provides a sensitive probe of the anisotropy of the potential. For methane, the effect of a magnetic field on the viscosity,[30–35] but not on diffusion, has been measured. In the presence of a magnetic field, the coupling between velocity and angular momentum is partially destroyed and the resulting changes in the viscosity are observed both parallel (longitudinal effects) and normal (transverse effects) to the direction of the field.[1,34]

Since methane is a spherical-top molecule, only the polarizations present for linear molecules, $\overline{\mathbf{jj}}$, $\overline{\mathbf{WWj}}$, and $\overline{\mathbf{WWjj}}$, need be considered.[1] The theoretical expressions in terms of relevant generalized cross sections have been derived for each polarization, but to the best of our knowledge, only in the spherical approximation (see Chap. 5.2.2 of Ref. 1). All the experimental evidence points to the dominance of the $\overline{\mathbf{jj}}$ contribution and all the analyses of the experimental data, to extract the appropriate generalized cross sections, have been performed on this basis. We are now in a position to assess the validity of this assumption by calculating the contributions from the other two polarizations and hence can test the validity of the experimental analyses based solely on the $\overline{\mathbf{jj}}$ contribution.

In the presence of a magnetic field, the changes in the viscosity coefficient, which is now a tensorial quantity, can be described in terms of five, nonzero, independent ratios:[1] three, $\Delta\eta_i^+/\eta$, $i=0,1,2$, describing the longitudinal effects, and two, η_i^-/η, $i=1,2$, describing the transverse effects. For conciseness, here we give an expression for one longitudinal viscomagnetic ratio only,

$$\frac{\Delta\eta_1^+}{\eta} = -\psi_{02}f(\xi_{02}) + \frac{5\psi_{21}}{4}f(\xi_{21}) - \frac{\psi_{22}}{24}[7f(\xi_{22}) + 6f(2\xi_{22})], \tag{6}$$

where $f(x)=x^2/(1+x^2)$, and we refer the reader to p. 322 of Ref. 1 for the similar expressions for the other four ratios. The dimensionless field parameter ξ_{pq} is given by

$$\xi_{pq} = \frac{g_{\mathrm{rot}}\mu_N k_B T}{\hbar\langle v\rangle_0}\frac{1}{\mathfrak{S}(pq00)_0}\frac{B}{P}. \tag{7}$$

Here, g_{rot} is the rotational g-factor, μ_N is the nuclear magneton, B is the magnetic flux density, and P is the pressure. The unbarred cross section $\mathfrak{S}(pq00)_0$ can be calculated as the weighted average of the related barred cross sections [see Eqs. (5.2–11) of Ref. 1].

The quantity ψ_{pq} in Eq. (6), which governs the magnitude of the contribution from each polarization, is given by

$$\psi_{pq} = \frac{\mathfrak{S}\binom{pq00}{2000}^2}{\mathfrak{S}(2000)\mathfrak{S}(pq00)_0}. \tag{8}$$

Knowledge of the values of the three pairs, (ξ_{02},ψ_{02}), (ξ_{21},ψ_{21}), and (ξ_{22},ψ_{22}), which characterize the $\overline{\mathbf{jj}}$,$\overline{\mathbf{WWj}}$, and $\overline{\mathbf{WWjj}}$ polarizations, respectively, is sufficient to describe all five viscomagnetic ratios.

When the $\overline{\mathbf{jj}}$ polarization is dominant, as has been assumed in previous analyses of the experimental data,[32–35] only three cross sections, $\mathfrak{S}(2000)$, $\mathfrak{S}(0200)$, and $\mathfrak{S}\binom{0200}{2000}$, govern the viscomagnetic effect. Then independent knowledge of the viscosity cross section, $\mathfrak{S}(2000)$, allows, after some judicious manipulation of the experimental viscomagnetic data, for the estimation of the other two: namely, $\mathfrak{S}(0200)$ and $|\mathfrak{S}\binom{0200}{2000}|$.

III. CLASSICAL TRAJECTORY CALCULATIONS

The classical-trajectory calculations were performed using an extension of the TRAJECT software code for linear molecules.[19] The linear-molecule program was utilized for the calculations performed for pure nitrogen,[3,6,36] carbon monoxide,[4–6,28] and carbon dioxide.[7–9,37] This code has been modified[20] to allow for the additional variables and averaging needed for asymmetric tops. The methane molecule was

represented as a rigid spherical top forming a regular tetrahedron with bond lengths of 0.1099 nm. For a given total energy, translational plus rotational, classical trajectories describing the collision of two molecules were obtained by integrating Hamilton's equations from pre- to postcollisional values. The initial values of the momenta for the relative motion and for the rotation of the two molecules, as well as the angles defining their relative orientation, were obtained using a pseudorandom number generator. The total-energy-dependent generalized cross sections can be represented as 13-dimensional integrals, which were evaluated by means of a Monte Carlo procedure.

The classical trajectories were determined at 29 values of the total energy, divided into three ranges. In each range the energy values were chosen as the pivot points for Chebyshev interpolation in order to facilitate calculations of the cross sections at a number of temperatures.[20,38] The highest energy used was 40 000 K, which is more than sufficient for the temperature range considered in this work. At each energy up to 1 000 000 classical trajectories were evaluated. The number of trajectories had to be reduced toward lower energies, those of the order of the well depth and smaller, because the low-energy trajectories require much longer computing times. For example, at 20 K, the lowest energy considered, only 20 000 trajectories were calculated. The precision of the calculations was assessed by estimating the convergence of the final temperature-dependent generalized cross sections as a function of the number of trajectories used. Furthermore, the symmetry of production cross sections under time reversal,

$$\mathfrak{S}\begin{pmatrix} p & q & s & t \\ p' & q' & s' & t' \end{pmatrix} = (-1)^{q+q'}\mathfrak{S}\begin{pmatrix} p' & q' & s' & t' \\ p & q & s & t \end{pmatrix},$$

allows the comparison between two cross sections calculated by two independent expressions. This was used as a further indicator of precision.

The classical trajectories have been evaluated using a recently developed six-dimensional *ab initio* intermolecular potential energy hypersurface.[14] To reduce the computational effort generating the surface, the CH_4 molecule was represented as a rigid spherical top. The form of the potential function is fully described in the original publication[14] and only the main characteristics will be summarized here.

Seventeen different angular orientations of the two methane molecules were considered with sixteen different center-of-mass separations for each orientation, resulting in 272 grid points. All calculations were performed within the counterpoise-corrected supermolecule approach at the CCSD(T) level of theory using the aug-cc-pVTZ and aug-cc-pVQZ basis sets. The resulting energies were extrapolated to the complete basis-set limit and an analytical site-site potential function, with nine sites per CH_4 molecule, was then fitted to the extrapolated interaction energies. (A spherical-harmonic expansion is not essential for a classical calculation.) A semiempirical correction for zero-point vibrational effects was also developed and incorporated into the final potential. This correction used only one adjustable parameter, chosen so that the calculated second pressure virial coefficient agreed with the best experimental value at room temperature. The resulting potential exhibits a maximum in the well depth of 286 K, occurring at a separation of 0.362 nm, see the discussion in Ref. 14. The spherically averaged potential has a well depth of 170 K at a separation of 0.420 nm. This new potential is the current state-of-the-art representation of methane-methane, attested by the excellent agreement with the available experimental second virial data over the temperature range of 160–620 K.[14]

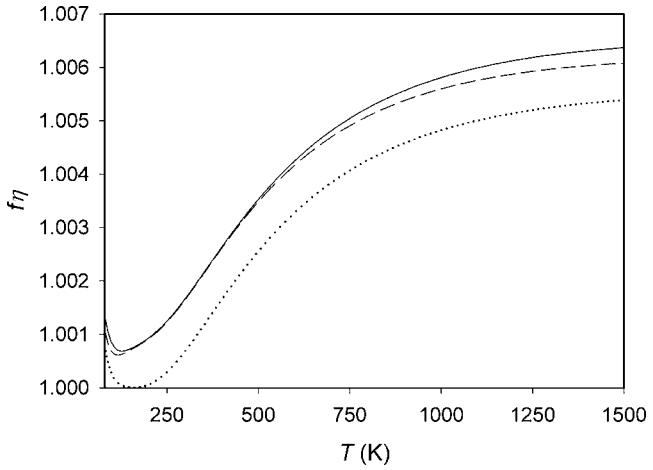

FIG. 1. Comparison of the values of the two second-order corrections: $f_\eta^{(2)}$ (----); $f_\eta^{(2')}$ (·····); and of the third-order correction $f_\eta^{(3)}$ (——), for the shear-viscosity coefficient.

IV. RESULTS

The calculations of the generalized cross sections were performed on a modern Linux workstation and took about 11 days of CPU time. The evaluation of the classical trajectories was the most time-consuming part in the computations.

All the calculated transport and relaxation cross sections are characterized by the customary monotonic decrease with temperature, while some of the production cross sections exhibit a maximum at low temperature. The values of the transport and relaxation cross sections are, on average, an order of magnitude larger than those of the production cross sections. Based on the convergence tests, the precision of most of the calculated transport and relaxation cross sections is estimated to be better than $\pm 0.1\%$, while the precision of most of the production cross sections is estimated to be better than $\pm 1.0\%$ at all except the very lowest temperatures.

Tables of all the generalized cross sections, and the shear viscosity and self-diffusion coefficients calculated in this work, have been deposited with the Electronic Physics Auxiliary Publication Service.[39]

A. Shear viscosity

1. Higher-order contributions

Before the comparison with experiment, we consider first the magnitude and temperature dependence of the higher-order contributions to the shear viscosity. Figure 1 illustrates the temperature dependence of the second- and third-order viscosity correction factors $f_\eta^{(2)}$, $f_\eta^{(2')}$, and $f_\eta^{(3)}$ (see Sec. II A).

Above temperatures of about 140 K, the magnitude of the higher-order correction factors increases with temperature, as shown in Fig. 1, reaching a saturation value at about 1400 K. The overall impact is small, however, and even at the highest temperature of the viscosity measurements[40] on methane (1050 K), the correction factor $f_\eta^{(3)}$ will contribute only 0.6% to viscosity. The contribution of the third order itself to the overall correction factor is very small, at most 0.04% in viscosity. The second-order correction factor shows a similar temperature dependence. Its magnitude is similar to that observed for nitrogen[36] and carbon monoxide,[4] but smaller than that found for carbon dioxide.[7]

By comparing the values of $f_\eta^{(2)}$ and $f_\eta^{(2')}$ (see Sec. II A) it can be seen that the angular-momentum coupling is responsible for at most 0.1% of the increase in the methane viscosity, this contribution being nearly independent of temperature. This angular-momentum coupling contribution is much smaller for methane than for any of the other three gases studied, consistent with the production cross section $|\mathfrak{S}(^{2000}_{0200})|$ being smaller for methane.

To account for the vibrational degrees of freedom, we have also corrected, using the methodology described in Ref. 8, the cross sections $\mathfrak{S}(^{20\,s\,t}_{20\,s't'})$ with $t+t' \neq 0$ that enter the higher-order correction factors. The overall impact is small, at most 0.01% in viscosity at the highest temperature studied.

2. Comparison with experiment

A critical evaluation of viscosity measurements on methane, based on the data available in 2000, was carried out[41] and used as the basis of a correlation in the limit of zero density, derived from experiments at low density. To derive values in the limit of zero density, either isothermal values as a function of density were extrapolated to this limit or individual values at low density were corrected to it using the Rainwater–Friend theory for the initial density dependence of the viscosity.[42–44] Near to room temperature the correlation was largely based on the experimental data by Schley *et al.*[45] available at the time, but published in 2004. These data, determined using a vibrating-wire viscometer in a relative manner for isotherms between 260 and 360 K (at 20 K intervals) up to maximum pressures of 29 MPa, are characterized by uncertainties of ±0.2% at low densities.

Since the development of this correlation, two groups have published new experimental data. Evers *et al.*[46] used a rotating-cylinder viscometer for absolute measurements between 233 and 523 K, up to pressures of 30 MPa, with uncertainties of the results at low densities estimated by the authors to be ±0.15%. For the comparison with theory, their low-density values were corrected to zero density, allowing for the initial density dependence of the viscosity.

The most recent measurements were carried out by May *et al.*[47] with single-capillary and two-capillary viscometers between 211 and 392 K at low densities in a manner that allowed direct extrapolation to the zero-density limit. They based their results for methane on zero-density viscosity values for helium in the same temperature range obtained from *ab initio* calculations using quantum mechanics and statistical mechanics,[48] particularly on a reference value for helium at 298 K at zero density $[\eta^{\mathrm{He}}_{0,298.15}=(19.833\pm0.016)\ \mu\mathrm{Pa\ s}]$,[49] derived from the best measurement (19.842 μPa s),[50,51] and the best *ab initio* calculations (19.8245 μPa s) known at that time.[48] Note that the viscosity values for helium used by May and co-workers[47,49] are in excellent agreement with analogous results calculated very recently by our group from *ab initio* calculations and the corresponding kinetic theory (19.8262 μPa s at 298.15 K).[52] This independent calculation lends support to the uncertainty of ±0.1% claimed by May *et al.*[47] for their experimental data in the complete temperature range.

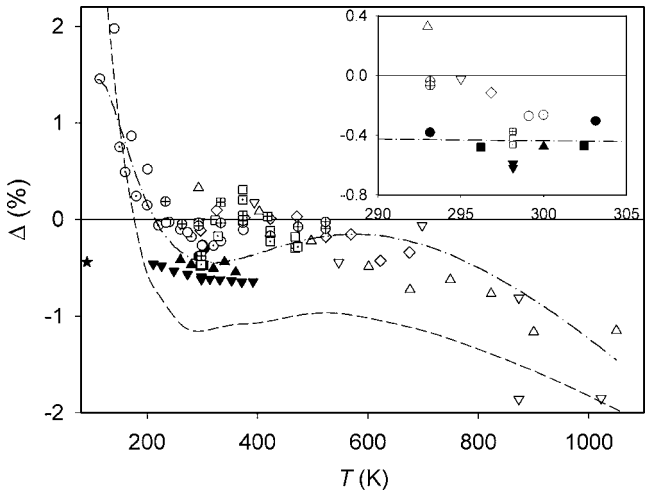

FIG. 2. Deviations of experimental zero-density viscosity coefficients from values theoretically calculated for CH_4. Deviations are defined as $\Delta=(\eta_{\mathrm{exp}}-\eta_{\mathrm{cal}})/\eta_{\mathrm{cal}}$. Experimental data: (●) Kestin and Yata (Ref. 53), (○) Clarke and Smith (Ref. 54), (△) Dawe *et al.* (Ref. 40), (■) Kestin *et al.* (Ref. 55), (□) Hellemans *et al.* (Ref. 56), (▽) Maitland and Smith (Ref. 57), (★) Slyusar *et al.* (Ref. 58), (◇) Timrot *et al.* (Ref. 59), (⊙) Gough *et al.* (Ref. 60), (⊡) Kestin *et al.* (Ref. 61), (⊞) Abe *et al.* (Ref. 62), (⊕) Evers *et al.* (Ref. 46), (▲) Schley *et al.* (Ref. 45), (▼) May *et al.* (Ref. 47). Experimentally based data: (–·–·–), values for the zero-density correlation of methane by Vogel *et al.* (Ref. 41); (----), values calculated by means of an isotropic potential (fitted to experimental data) by Zarkova *et al.* (Ref. 63).

The comparison between the results of the best available measurements[40,45–47,53–62] and the values calculated using the new intermolecular potential surface of methane is illustrated in Fig. 2. The results at ambient temperature, additionally shown in the inset of the figure, provide an accurate and a distinct experimental data set.

The figure demonstrates that the experimental data of May *et al.*,[47] measured in the temperature range of 210–390 K, deviate from the calculated values by −(0.52 to 0.66)%. This indicates that either the rigid-rotor assumption needs to be relaxed or the intermolecular potential needs some minor improvement. Nevertheless, it reveals also that the potential reproduces appropriately the temperature dependence of the viscosity in this temperature range. Over a more limited temperature range, 260–360 K, the temperature dependence of the viscosity data of Schley *et al.*[45] is consistent with that of the experiments by May *et al.*,[47] although the values of Schley *et al.*[45] are higher by about 0.1%. This difference arises because Schley *et al.*[45] used an

old reference value for the viscosity of argon[64] for the calibration of their vibrating-wire viscometer at room temperature.

Experimental data reported by Kestin and co-workers[53,55,56,61,62] differ at ambient temperature from the values of May *et al.*[47] by about +(0.1 to 0.2)%. However, at temperatures between 320 and 380 K the experimental data of Kestin and co-workers,[56,61,62] estimated uncertainty less than ±0.3%, deviate from the experiments of May *et al.*[47] by up to +0.9%. Although the values at higher temperatures agree better with the calculated values for the potential surface of methane, they are definitely incorrect. The differences from the reliable data of May *et al.*[47] and Schley *et al.*[45] are due to a temperature measurement error in the experiments of Kestin and co-workers with their high-temperature oscillating-disk viscometer.[65] This error was extensively discussed by Vogel *et al.*[44] and was confirmed by comparison of standard viscosity values for helium[52] and neon,[66] obtained from *ab initio* calculations and using the appropriate kinetic theory, with viscosity data of these gases measured by Kestin and co-workers using the same viscometer.

Figure 2 illustrates also that the experimental values of Evers *et al.*[46] are too high by about 0.5%–0.6% compared to the experimental data of May *et al.*,[47] Schley *et al.*,[45] Kestin and Yata,[53] and Kestin *et al.*[55] Although the results of the measurements on helium and neon reported by Evers *et al.*[46] in the same paper are in excellent agreement with the reliable data of other investigators (see Refs. 52 and 66), for methane this is not the case. Hence, their agreement with the calculated values is most likely fortuitous.

The experimental values of Smith and co-workers,[40,54,57,60] obtained from relative measurements with capillary viscometers, reveal a characteristic behavior when compared with the calculated values at low and at high temperatures. The differences for the data by Clarke and Smith,[54] as well as by Gough *et al.*,[60] increase by about +(1.0 to 1.5)% with decreasing temperature down to 150 K. On the contrary, the data of Dawe *et al.*,[40] as well as of Maitland and Smith,[57] are too high by 1% at room temperature and too low by about 1% at 1000 K. Similar differences were found for the viscosity data of this group in the case of helium and neon (see again Refs. 52 and 66). The lower accuracy of these data makes them unsuitable for the validation of the *ab initio* potential energy surface.

The viscosity correlation in the limit of zero density proposed by Vogel *et al.*[41] (shown in Fig. 2) displays increasing deviations from the calculated values both at low and high temperatures, consistent with the behavior of the experimental data which were used to generate the correlation. As has already been discussed, these data are of lower accuracy than the calculated values.

We believe that the present calculations provide the best estimate of the viscosity of methane at temperatures lower than 200 K. At temperatures up to 400 K, the calculated values are characterized by nearly the same temperature dependence as the experimental data of May *et al.*[47] Hence, we expect that the calculated values exhibit the proper temperature dependence also for temperatures above 400 K, unlike most of the experimental data. Based on the comparison with the available data, especially around room temperature, we estimate the uncertainty of the computed values to be of the order of ±1% at 80 and 1500 K.

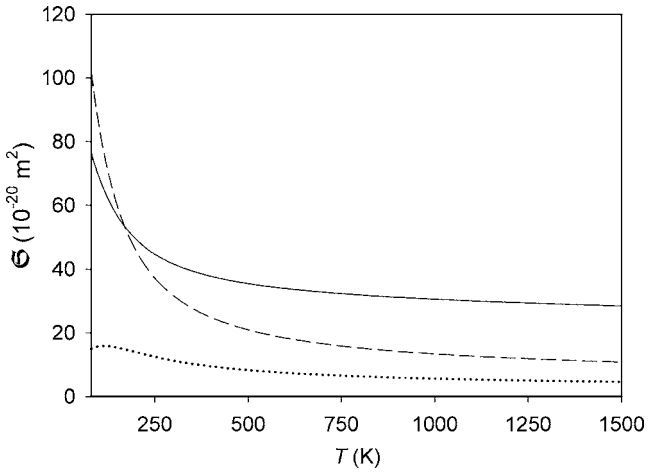

FIG. 3. Comparison of the values of the generalized cross sections $\mathfrak{S}(2000)$ (——); $\mathfrak{S}(0200)$ (----), and $10\times\mathfrak{S}\left(^{0200}_{2000}\right)$ (·····).

Finally, Fig. 2 also shows a comparison with values recommended as reference data by Zarkova *et al.*[63] These values were calculated via an isotropic three-parameter Lennard-Jones $(n-6)$ potential obtained from a multiproperty fit to experimental data for the second pressure and acoustic virial coefficients, as well as for viscosity and self-diffusion at low density. They agree neither with the calculated values nor with the experimental data and hence cannot be considered as standard viscosity values for methane.

B. Viscomagnetic effects

1. Relevant cross sections

In order to compare with the experimental data we have calculated the values of the relevant viscomagnetic coefficients in two ways. First, we employed the full expressions [see, for example, Eq. (6)] that include the contributions of all three polarizations, and second we made use only of the terms corresponding to the dominant $\overline{\mathbf{jj}}$ polarization.

Figure 3 illustrates the temperature dependence of the three cross sections that govern the viscomagnetic effect, assuming that the $\overline{\mathbf{jj}}$ polarization is dominant. All three cross sections decrease with increasing temperature, most markedly at low temperatures. At temperatures below about 175 K, the $\mathfrak{S}(0200)$ cross section, which describes the relaxation/decay of the angular-momentum polarization, is larger than the viscosity cross section $\mathfrak{S}(2000)$, while at high temperatures the reverse is true. Hence, a relaxation of angular momentum is more favorable than exchange of linear momentum at lower temperatures. The production cross section is about one to two orders of magnitude smaller than the cross sections $\mathfrak{S}(0200)$ and $\mathfrak{S}(2000)$, indicating that collisions are ineffective in coupling the angular-momentum polarization to that in velocity.

The cross sections that govern the $\overline{\mathbf{WWj}}$ and $\overline{\mathbf{WWjj}}$ polarizations show similar qualitative features to those seen in Fig. 3. Since the relaxation cross sections $\mathfrak{S}(pq00)_0$ for all

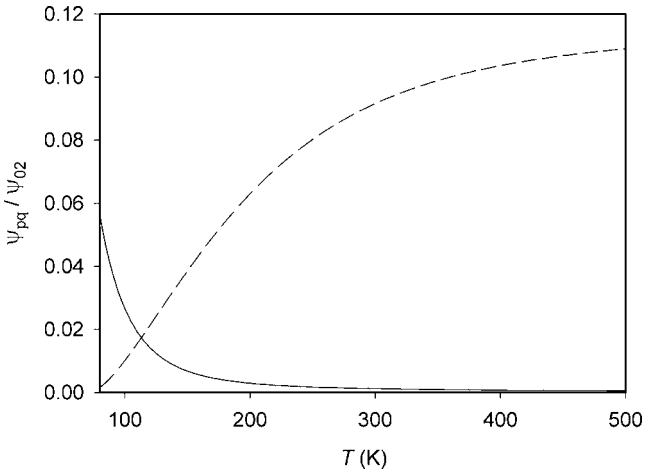

FIG. 4. Ratios of the viscomagnetic parameters ψ_{pq}/ψ_{02} for $pq \equiv 21$ (----) and $pq \equiv 22$ (——) as a function of temperature.

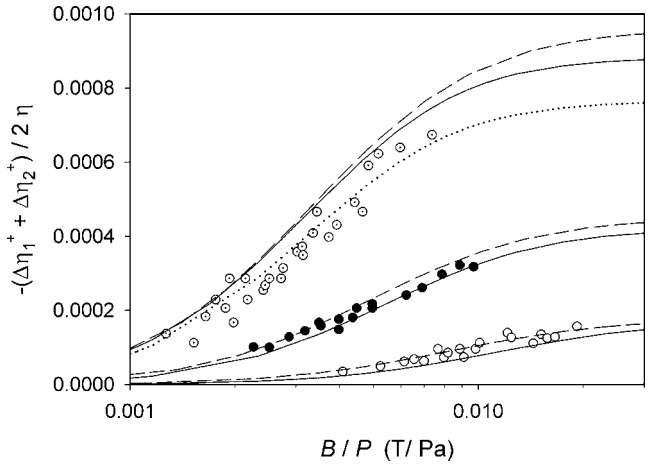

FIG. 5. Comparison of the measurements of Burgmans *et al.* (Ref. 35) of the viscomagnetic effect $-(\Delta\eta_1^+ + \Delta\eta_2^+)/2\eta$ with the present calculations. Experimental values: (○), 154 K; (●), 224 K; (⊙), 293 K. To distinguish between the curves for the different temperatures they are vertically shifted by dividing them by 4, 2, and 1, respectively. Calculations: (----), **jj** polarization only; (——), full calculation; (·····), full calculation with the value of the $\mathfrak{S}\binom{0200}{2000}$ cross section reduced by 6%.

three polarizations are comparable, the contribution of each polarization to the viscomagnetic effect is driven primarily by the magnitude of $\mathfrak{S}\binom{pq00}{2000}$. Figure 4 illustrates the temperature dependence of the ratios ψ_{pq}/ψ_{02}, $pq=21,22$. As these ratios are small over most of the range studied, we can conclude that the **jj** polarization is indeed dominant. However, at low temperature some influence of the **WWjj** polarization will be present, while at high temperature, dominated by contributions from the repulsive part of the potential surface, there will be a small contribution of the **WWj** polarization to the viscomagnetic coefficients. Because of cancellations between the different contributions to the observables [see Eq. (6)], some viscomagnetic coefficients are more sensitive to the secondary polarizations than the relatively small values of these ratios would suggest.

2. Comparison with experiment

Six independent measurements of viscomagnetic effects in methane,[30–35] carried out in two different laboratories, have been performed using capillary viscometers operating in a null mode. Korving and co-workers[30,31] were the first to report that methane gas exhibits a viscomagnetic effect. They carried out the measurements of the sum of two longitudinal coefficients, $-(\Delta\eta_1^+ + \Delta\eta_2^+)/2\eta$, at room temperature at values of the magnetic flux density over pressure (B/P) of up to 0.004 T/Pa (≡5.4 kOe/torr). We have not used these data in our analysis as they are in good agreement with the later work[35] that reports the experimental data for the same combination of the longitudinal coefficients over a larger range of (B/P) values.

Hulsman *et al.*[32] carried out measurements on the transverse coefficients at room temperature at (B/P) values up to 0.005 T/Pa (≡7 kOe/torr). Korving[33] measured, also at room temperature but with a stronger magnet, two longitudinal coefficients, $-\Delta\eta_1^+/\eta$ and $-(\Delta\eta_2^+ - \Delta\eta_1^+)/\eta$, at (B/P) values of as high as 0.024 T/Pa (≡32 kOe/torr). Subsequently, Hulsman *et al.*[34] performed a further set of measurements to evaluate the longitudinal coefficients at room temperature in the (B/P) range up to 0.007 T/Pa (≡9.6 kOe/torr). They used an experimental arrangement with an electromagnet that could be rotated to realize different orientations between the magnetic field and the flow. Measurements at three different orientations allowed them to evaluate $-\Delta\eta_0^+/\eta$, $-\Delta\eta_1^+/\eta$, and $-(\Delta\eta_2^+ + \Delta\eta_0^+)/2\eta$. Finally, Burgmans *et al.*[35] measured the sum of two longitudinal coefficients, $-(\Delta\eta_1^+ + \Delta\eta_2^+)/2\eta$, at three temperatures, 154, 224, and 293 K, for (B/P) values of up to 0.02 T/Pa (≡25 kOe/torr).

Of these six experiments, only that of Hulsman *et al.*[34] measured the value of $-\Delta\eta_0^+/\eta$. This ratio is the one ratio vanishing for a **jj** polarization[1] and hence is expected to be much smaller than the other four ratios.

By examining the variation of the viscosity coefficients as a function of (B/P), the four more recent studies concluded that **jj** polarization was dominant and used this as the basis of their analyses. They extracted the relevant cross sections $\mathfrak{S}(0200)$ and $|\mathfrak{S}\binom{0200}{2000}|$ by fitting the theoretical expressions, such as Eq. (6), to the (B/P) dependence of their observations, treating the values of these two cross sections as adjustable parameters. For this purpose, Burgmans *et al.*[35] used the experimental data over the whole measured (B/P) domain, while Hulsman and co-workers[32,34] and Korving[33] preferred a fit that gave more weight to the measurements at lower values of (B/P).

Figures 5–8 show the comparison between the calculated values of the viscomagnetic coefficients and the available experimental data (read from the published figures). No uncertainty estimate is given by the authors for the experimental data, although it is stated[34] that relative viscosity changes of 2×10^{-6} could be detected.

We start by comparing the calculated values to the data of Korving[33] and Burgmans *et al.*,[35] both sets of workers having measured the longitudinal viscomagnetic coefficients. The agreement with the data of Burgmans *et al.*[35] (Fig. 5) is, in general, good, although the calculated values overestimate the data at room temperature, particularly at the lower (B/P) values. This is in contrast to the comparison with the experi-

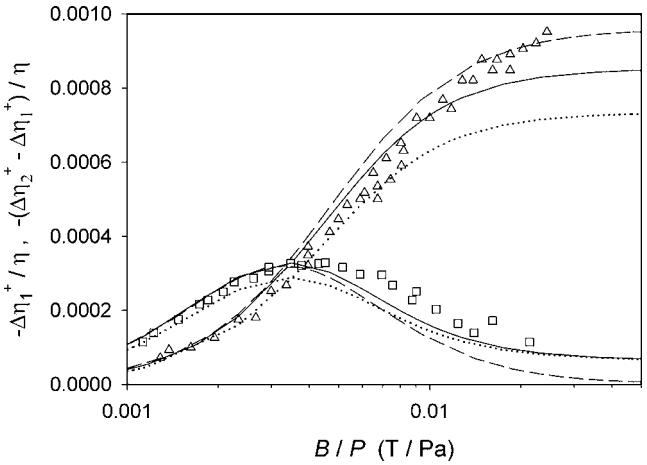

FIG. 6. Comparison of the measurements of Korving (Ref. 33) at 293 K of the viscomagnetic effect with the present calculations: (△), $-\Delta\eta_1^+/\eta$ and (□), $-(\Delta\eta_2^+-\Delta\eta_1^+)/\eta$. Calculations: (----), $\overline{\mathbf{jj}}$ polarization only; (——), full calculation; and (·····), full calculation with the value of the $\mathfrak{S}\binom{0200}{2000}$ cross section reduced by 6%.

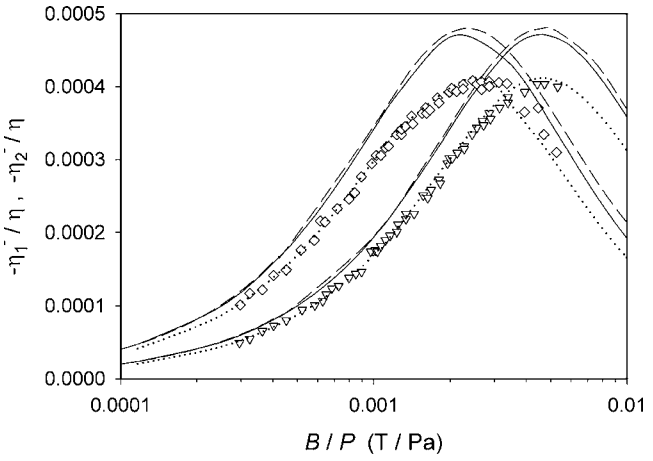

FIG. 8. Comparison of the measurements of Hulsman *et al.* (Ref. 32) at 293 K of the viscomagnetic effect with the present calculations: (▽), $-\eta_1^-/\eta$ and (◇), $-\eta_2^-/\eta$. Calculations: (----), $\overline{\mathbf{jj}}$ polarization only; (——), full calculation; and (·····), full calculation with the value of the $\mathfrak{S}\binom{0200}{2000}$ cross section reduced by 6%.

mental data of Korving[33] at room temperature for different combinations of longitudinal coefficients, as shown in Fig. 6. In the (B/P) range corresponding to the observations of Burgmans *et al.*[35] only a slight overestimate is observed, while at high (B/P) values, a slight underestimate occurs. The calculations predict well both the (B/P) dependence and the magnitude of the measured coefficients.

Figure 7 illustrates the comparison between the calculated values and the experimental data of Hulsman *et al.*[34] Excellent agreement is observed for the $-\Delta\eta_0^+/\eta$ ratio, which is very encouraging as for this ratio the normally dominant $\overline{\mathbf{jj}}$ polarization does not contribute and only the $\overline{\mathbf{WWj}}$ and $\overline{\mathbf{WWjj}}$ polarizations contribute; the former, $\overline{\mathbf{WWj}}$, being the more important. The agreement with experimental data pertaining to the $-\Delta\eta_1^+/\eta$ ratio is also very good, with a slight overestimate at high (B/P) values. However, the computed values overestimate the combination $-(\Delta\eta_2^+ + \Delta\eta_0^+)/\eta$. This may not be surprising since the values of the combination

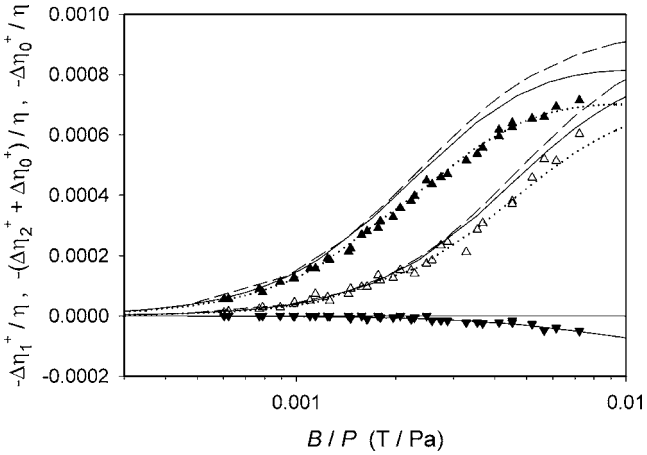

FIG. 7. Comparison of the measurements of Hulsman *et al.* (Ref. 34) at 293 K of the viscomagnetic effect with the present calculations: (△), $-\Delta\eta_1^+/\eta$; (▲), $-(\Delta\eta_2^+ + \Delta\eta_0^+)/\eta$; and (▼), $-\Delta\eta_0^+/\eta$. Calculations: (----), $\overline{\mathbf{jj}}$ polarization only; (——), full calculation; and (·····), full calculation with the value of the $\mathfrak{S}\binom{0200}{2000}$ cross section reduced by 6%.

$-(\Delta\eta_1^+ + \Delta\eta_2^+)/2\eta$ derived from the experimental data of Hulsman *et al.*[34] are consistent with the room temperature data of Burgmans *et al.*[35] Hence, the overestimate observed in Figs. 5 and 7 is primarily due to the overestimate of the $-\Delta\eta_2^+/\eta$ ratio.

The significance of the overestimation of the room-temperature data of Burgmans *et al.*[35] is better seen when comparing the calculations with the data of Hulsman *et al.*[32] (see Fig. 8), pertaining to the two transverse coefficients. We predict well the (B/P) dependence of the curves and the position of both maxima, but not the magnitude of the peaks. Hence, the overestimation of both the experimental data of Burgmans *et al.*[35] and of Hulsman *et al.*[32] at 293 K can be attributed to the magnitude of the calculated production cross section $\mathfrak{S}\binom{0200}{2000}$ being too large.

In fact, if we reduce the calculated value of this cross section by 6%, the agreement with the experimental data from both experiments[32,35] would be essentially perfect, as illustrated in Figs. 5, 7, and 8. However, the agreement with the data of Korving[33] would become worse, especially for the $-(\Delta\eta_2^+ - \Delta\eta_1^+)/\eta$ ratio, as illustrated in Fig. 6. It is not clear which data set is the more accurate, but at present it appears unlikely that the error in the anisotropy of the proposed methane potential is such that the production cross section at room temperature would be in error by 6%. However, the evidence of additional anisotropy-sensitive properties needs to be assessed before any firm conclusions can be drawn. Also, it should be borne in mind that the accuracy of neither the lowest-order kinetic theory nor of the spherical approximation used for analyzing these experiments has ever been assessed.

The calculations of the viscomagnetic coefficients based on the truncated expressions that include only the $\overline{\mathbf{jj}}$ polarization are generally in good agreement with the full calculations. Within the experimental temperature and (B/P) range studied, the secondary polarization is at most at the 5% level, hence supporting the experimentally based observation that the $\overline{\mathbf{jj}}$ polarization is dominant. The only exception is the combination of two longitudinal coefficients measured by

Korving[33] and Hulsman *et al.*[34] Figure 6 illustrates that at high (B/P) values the **WWj** polarization becomes significant, especially when the difference of two viscomagnetic coefficients is measured. In this case, at the highest (B/P) value measured (0.024 T/Pa), the **WWj** polarization contributes about 12%.

The excellent agreement between the calculated and the measured values for these coefficients, together with excellent agreement with the results of Hulsman *et al.*[34] for the $-\Delta\eta_0^+/\eta$ ratio, gives further support to the accuracy of the potential surface. In the latter case, a combination of five cross sections was required to predict the viscomagnetic effect, although a fortuitous cancellation of errors cannot be discounted.

Hulsman and co-workers,[32,34] Korving,[33] and Burgmans *et al.*[35] have all made use of their data, with the assumption of only **jj** polarization, to evaluate the $\mathfrak{S}(0200)$ cross section at 293 K. The values obtained range[32–35] from 30 to 33.0 Å^2, with error bars[35] of ±2.5 Å^2. Our calculated value is 32.3 Å^2, in excellent agreement with the experimental values. At 224 K, our calculated value of 41.2 Å^2 is again in excellent agreement with the experimental value[35] of 40±3 Å^2. At the lowest temperature (154 K), the calculated value of 58.3 Å^2 is outside the error limits of the value obtained from the experiments,[35] 67±5 Å^2. However, the comparison is misleading. In order to extract the value of $\mathfrak{S}(0200)$ from the experimental data, $\mathfrak{S}(0200)$ was treated as one of the two adjustable parameters. The (B/P) range of the experimental data, all far from the peak, is such that it does not allow for a unique determination of the two cross sections, rather a number of different combinations will give reasonably good fits, as our calculated values attest (see Fig. 5). So, in this case the comparison at the cross-section level is not appropriate.

Burgmans *et al.*[35] quoted the values of the production cross sections $|\mathfrak{S}(^{0200}_{2000})|$, with uncertainties of about 6%. At both 293 and 224 K, the calculated values are just outside their uncertainties, while at 154 K, as already discussed, it is not sensible to make such a comparison.

C. Self-diffusion

There have been measurements[67,68] of the diffusion of isotopomers of methane (excluding those involving deuterium or tritium) that have been used to infer the self-diffusion coefficient of methane. We recall that for a spherical potential the classical diffusion cross section, for a specified potential, is independent of the reduced mass of the interacting particles. Hence, differences between the various isotopomers can arise only due to the anisotropic part of the potential surface. Since the substitution of ^{13}C for ^{12}C does not change the moment of inertia of CH_4, the calculation of $\mathfrak{S}'(1000)$ should be particularly insensitive to this substitution.

Using mass spectrometry, Winn and Ney[67] measured the diffusion of $^{13}CH_4$ in $^{12}CH_4$ at room temperature with an estimated uncertainty of ±2.7%. Later, using the same technique, Winn[68] made measurements over the temperature range of 90–353 K, with an uncertainty estimated at ±2% at and above room temperature, but up to ±8% at the lowest temperature. Both sets of results that were reported included a correction[69] for the effect of the mass difference between $^{13}CH_4$ and $^{12}CH_4$ on $\langle v\rangle_0$ [see Eq. (2)].

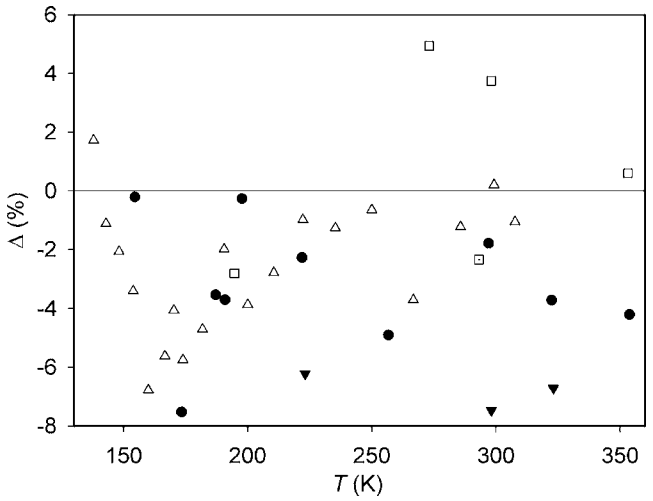

FIG. 9. Deviations of experimental self-diffusion coefficients from values theoretically calculated for CH_4. Deviations are defined as $\Delta=[(nmD_{exp,0})/(nmD_{cal,0})-1]$. Experimental data: (⊡) Winn and Ney (Ref. 67), (□) Winn (Ref. 68), (●) Dawson *et al.* (Ref. 70), (△) Oosting and Trappeniers (Ref. 71), and (▼) Harris (Ref. 72).

In addition to these measurements using isotopically labeled molecules, there are also results available for self-diffusion in $^{12}CH_4$ from NMR spin-echo experiments.[70–72] We are unaware of any kinetic-theory analysis beyond first order for this type of measurement. The NMR measurements of Dawson *et al.*[70] span from 155 to 354 K and their own estimate of the total uncertainty is ±6%, while the measurements of Oosting and Trappeniers[71] cover the range from 138 to 308 K with uncertainty estimated[73] as ±2%. As neither of these NMR experiments explicitly extrapolated their density-dependent results to the limit of zero density, we have made the extrapolation.

Harris[72] performed measurements at 223.15, 298.15, and 323.15 K. We have refitted the density dependence of these measurements and hence extrapolated to the zero-density limit. Harris[72] notes that when account is taken of the differences in calibration and of mutual uncertainties, the three sets of NMR measurements[70–72] are consistent.

Theory and experiment are compared in Fig. 9. The room-temperature measurement of Winn and Ney[67] is consistent with the calculated values. The measurement of Winn[68] at 90 K, estimated uncertainty ±8%, has been omitted from Fig. 9 as the deviation was very large, about 25%. Winn[68] commented that, due to the low density required, some difficulties were encountered in making measurements at this temperature. For helium-nitrogen mixtures, rotor constant of 2 cm^{-1} and only even changes in j allowed, the difference between classical and quantal results at 100 K was only 0.7%.[10] Hence, while quantal effects in methane, rotor constant of 5.25 cm^{-1}, are becoming more significant at 90 K, these effects are unlikely to explain the 25% deviation. The data of Winn[68] at higher temperature, 195–353 K, are

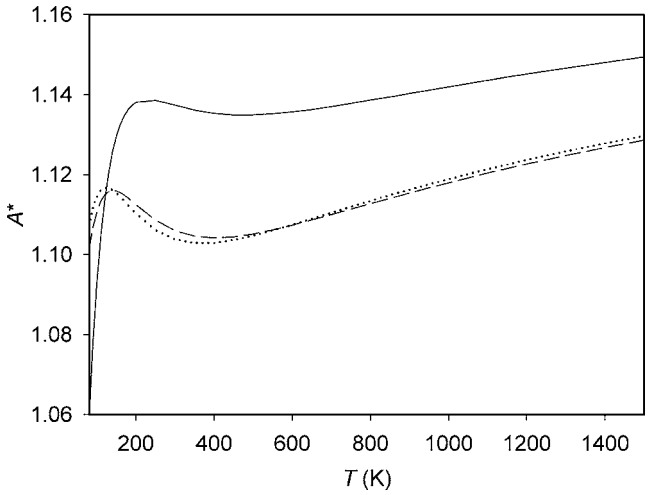

FIG. 10. Comparison of calculated values for the dimensionless parameter A^* [see Eq. (5)] as a function of temperature: (——), classical trajectories (CT): (----), Mason-Monchick approximation (MMA); and (·····), spherical-potential approximation (SPA).

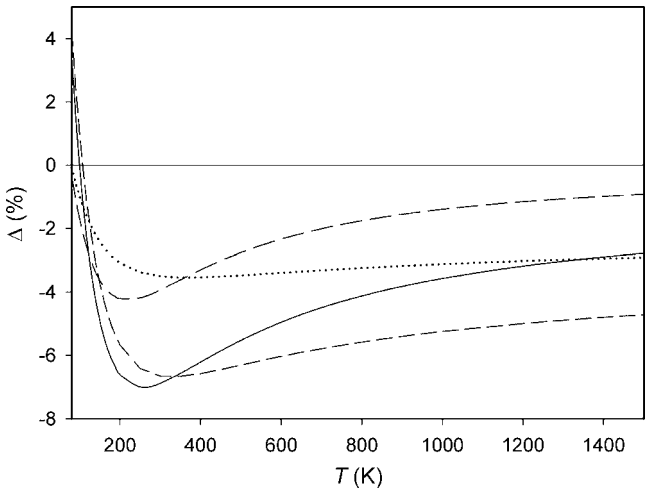

FIG. 11. Deviations of the values of generalized cross sections calculated using the Mason-Monchick approximation (MMA) and the spherical-potential approximation (SPA) from values obtained with classical trajectories (CT). Deviations defined as $\Delta=(\mathfrak{S}_{CT}-\mathfrak{S}_{approx})/\mathfrak{S}_{CT}$. (——), MMA $\mathfrak{S}'(1000)$, (– – –), MMA $\mathfrak{S}(2000)$, (----), SPA $\mathfrak{S}'(1000)$, and (·····), SPA $\mathfrak{S}(2000)$.

broadly in agreement with the calculated values, but the deviations are up to twice his estimated uncertainty.

Apart from the measurement at 173 K, the measurements of Dawson *et al.*[70] are consistent with theory. For the data of Oosting and Trappeniers,[71] the differences are generally rather larger than the authors' uncertainties, although the agreement at temperatures higher than 223 K is reasonable, with deviations just outside the quoted uncertainties. The most recent observations, those of Harris,[72] lie about 7% below our calculated values.

Comparisons with measurements of self-diffusion in CD_4 and other isotopomers will be considered in a separate publication.

Figure 10 illustrates the temperature dependence of the calculated value of the A^* parameter, as defined by Eq. (5). The value of A^* initially increases rapidly with temperature, reaching a value of 1.14 at about 250 K. The subsequent change with increasing temperature is slow and A^* reaches a value of 1.15 at 1500 K.

It is interesting to note that there is no evidence of the leveling off with increasing reduced temperature observed for the other molecular gases studied.[4,7,36] However, the magnitude of A^* for methane and its temperature variation are in line with what has been observed for nitrogen,[28] carbon monoxide,[28] and carbon dioxide.[7]

D. Approximate methods

Until the advent of fast classical-trajectory calculations, it was not possible to compute transport properties without approximating either the dynamics of the collision or the intermolecular potential surface. The two most common approximations were (i) use of Mason–Monchick/infinite-order-sudden-type methods and (ii) use of only the spherical component of the intermolecular potential. It is of interest to examine the reliability of these approximations for estimating the viscosity and self-diffusion coefficients of a spherical top such as methane.

1. Mason–Monchick approximation

The MMA (Refs. 15 and 16) with quantal analog the infinite-order sudden approximation (IOSA),[17] has a long history and has been tested most recently for the calculation of the viscosity of carbon dioxide.[37] The MMA/IOSA approximates the dynamics of the binary collision by making two physically reasonable assumptions:[15–17,74,75] (i) the amount of rotational energy exchanged between the molecules is, on average, much smaller than the relative kinetic energy of the pair; and (ii) the relative orientation of the molecules can be treated as fixed during the part of the collision that is dominant in determining transport properties. Invoking both these assumptions, one can express the viscosity and self-diffusion generalized cross sections as averages over all possible orientations of the corresponding monatomic collision integrals,[22] evaluated at fixed orientation.

We have performed the MMA calculations for both the $\mathfrak{S}(2000)$ and $\mathfrak{S}'(1000)$ generalized cross sections, as described in Ref. 37, but with additional averaging for the spherical-top potential surface. Figure 11 illustrates the deviations from the CT values of the cross sections evaluated using the MMA. At low temperatures the cross sections evaluated by the MMA/IOSA decrease marginally more slowly with temperature than the corresponding CT values. This leads at low values of T^* to the underestimation of the CT cross sections by the MMA cross sections followed, at around $T^*=0.5-0.6$, by an overestimation. Here, T^* is the usual reduced temperature, given by $T^*=k_BT/\epsilon$, where ϵ is the well depth of the spherical component of the interaction. At higher reduced temperatures the deviations, as expected, become progressively smaller. The maximum deviations observed for the $\mathfrak{S}(2000)$ and $\mathfrak{S}'(1000)$ cross sections are −4.2% and −7.0%, respectively.

Similar trends have been observed for the other molecules studied: N_2,[76] CO,[28] and CO_2.[37] The deviations, defined as $\Delta'(2000)$ (see Ref. 37), decrease with decreasing anisotropy of the intermolecular potential. Among the four

gases studied, methane has the smallest anisotropy, as measured by the value of the rotational relaxation number. Hence, in the high-temperature limit, methane exhibits the smallest deviations. For instance, at 1000 K the rotational relaxation numbers for CO_2, CO, N_2 and CH_4 are 2.6, 4.4, 5.3, and 13.1, respectively,[37,77] while the $\Delta'(2000)$ values are −15.0%, −10.8%, −7.6%, and −3.9%, respectively. That methane possesses the smallest anisotropy is also consistent with the calculations of the contribution of the angular-momentum coupling to the second-order correction for the viscosity discussed in Sec. IV A.

In addition, the larger error in the MMA values for $\mathfrak{S}'(1000)$ cross sections than for $\mathfrak{S}(2000)$ cross sections has been observed previously[28,37,76] in molecular gases and in atom-molecule mixtures, see, for example, Ref. 78.

Figure 10 shows the values of the ratio A^* [see Eq. (5)] evaluated by the MMA, and the values obtained by the CT calculations. The MMA values of A^* are, on average, 1.4%–3% lower, the deviations decreasing slightly with temperature.

The MMA calculation has also been used to approximate the second-order correction factor for viscosity $f_\eta^{(2')}$ (see Sec. II A). This small correction mimics the behavior of the corresponding CT value illustrated in Fig. 1, attaining a value of 1.006 at 1500 K. The differences in the value of the second-order correction factor between the two calculations are 0.1% at most.

In the MMA, the second-order viscosity correction factor reduces to the monatomic result.[28] Hence, one would expect the corresponding second-order self-diffusion correction factor $f_D^{(2')}$, not yet derived for molecular gases, also to reduce to the monatomic result. We have made use of this assumed limiting behavior to estimate the value of $f_D^{(2')}$ using the MMA. This correction shows very similar temperature dependence to its viscosity counterpart, attaining a value of 1.006 at 1500 K. Given that the experimental values of the self-diffusion coefficient have an accuracy of the order of ±2% at best, see Sec. IV C, the second-order correction for self-diffusion can be neglected, if our assumptions are indeed satisfied.

2. Spherical approximation

We have also calculated the viscosity and self-diffusion generalized cross sections using only the spherical average of the full intermolecular potential surface. The deviations of the values obtained using the spherically averaged potential from the CT values, shown in Fig. 11, follow the same trends as those shown for the MM approximation, also included in the figure. The deviations have maximum values for $\mathfrak{S}(2000)$ and $\mathfrak{S}'(1000)$ of −3.5% and −6.6%, respectively, and remain approximately constant in the high-temperature limit. The temperature dependences of the deviations for both cross sections are very similar to those obtained using the MMA (see Fig. 11). At low temperatures, both cross sections obtained using the spherically averaged potential are 1.0% below the equivalent MMA values, while at high temperatures they overestimate the MMA values by 2.0%. Using the spherical approximation to evaluate A^*, the deviations from the CT values are almost indistinguishable from those obtained in the MM approximation (see Fig. 10).

V. SUMMARY AND CONCLUSIONS

We have performed the first calculations of the shear viscosity, viscomagnetic effects, and self-diffusion using a full anisotropic rigid-rotor methane-methane potential energy hypersurface. The classical-trajectory method has been employed to evaluate the generalized cross sections required in the best available kinetic theory.

For the shear viscosity, existing kinetic theory[4,25,27] has been extended to include third-order contributions. The comparison with the most accurate experimental data by May *et al.*[47] shows relatively constant deviations of −0.5% to −0.7% in the temperature range of 210–390 K, indicating that the temperature dependence of the viscosity is very well described by the calculations. This allows accurate extrapolations of the viscosity to temperatures outside the range of the measurements by May *et al.*[47] We estimate that the uncertainty of the computed viscosity values is approximately ±1% at 80 and 1500 K.

The difference between the third-order and second-order correction factors to the shear viscosity was found to be very small, below 0.04%, suggesting that the second-order results are adequate for comparison with current experiments or applications. Velocity-coupling contributions[27] dominated the angular-momentum–coupling contributions[25] to second-order effects, which in total never exceeded 0.65%.

The viscomagnetic effects are due to angular-momentum transfer and hence probe directly the anisotropic part of the potential surface. For these effects, the contributions from the three most likely polarizations[1] ($\mathbf{jj}$, $\overline{\mathbf{WW}}\mathbf{j}$, and $\overline{\mathbf{WW}}\mathbf{jj}$) have been investigated, although previous analyses of the measurements[30–35] have concentrated on the $\mathbf{jj}$ polarization. While this polarization was indeed found to be dominant, the contribution of the $\overline{\mathbf{WW}}\mathbf{j}$ polarization was observed at high values of (B/P), indicating that for the accurate analysis of the experimental data both polarizations need to be considered. Overall, the agreement with the measurements[32–35] was generally reasonable, bearing in mind that no information on the experimental uncertainty was available and that experimental data from different laboratories were not entirely consistent. The general (B/P) dependence and the position of the maxima for the transverse coefficients were predicted well, but in a number of instances, the magnitude of the viscomagnetic effect was overestimated. It is difficult at this stage to attribute the observed overestimate to the uncertainty in the anisotropy of the potential rather than to uncertainties in the experimental data, or the first-order kinetic theory employed in the analysis, as additional anisotropy-sensitive properties are currently being evaluated.[77]

The experimental data for self-diffusion are characterized by much larger differences from the calculated values than occurred for the shear viscosity. This behavior is due to the difficulties of the measurements, resulting in uncertainties estimated by the authors to be between ±2% and ±8%. The comparison illustrates that some of these estimates may still be overoptimistic. Hence, the experimental data do not

provide a critical test of the potential energy surface. The calculated self-diffusion coefficients, even without higher-order corrections, should be distinctly more reliable than the experimental data.

The parameter A^* attains a value in the range of 1.14–1.15 above room temperature, displaying a weak temperature dependence in line with the other gases studied. The viscosity and self-diffusion cross sections were also evaluated by means of the MM/IOS approximation.[15–17] The differences observed are smaller than those occurring for the linear molecules N_2,[76] CO,[28] and CO_2,[37] consistent with the methane potential surface being less anisotropic. Use of only the spherical component of the full potential surface provides estimates of the viscosity and self-diffusion cross sections comparable with the MMA/IOSA values.

ACKNOWLEDGMENTS

This work was financially supported by the German Research Foundation (Deutsche Forschungsgemeinschaft), Grant No. VO 499/14–1.

[1] F. R. W. McCourt, J. J. M. Beenakker, W. E. Köhler, and I. Kučšer, *Nonequilibrium Phenomena in Polyatomic Gases* (Oxford Science, Oxford, 1990), Vol. 1.
[2] A. K. Dham, F. R. W. McCourt, and A. S. Dickinson, J. Chem. Phys. **127**, 054302 (2007).
[3] E. L. Heck and A. S. Dickinson, Mol. Phys. **81**, 1325 (1994).
[4] E. L. Heck and A. S. Dickinson, Physica A **217**, 107 (1995).
[5] E. L. Heck and A. S. Dickinson, Physica A **218**, 305 (1995).
[6] E. Bich, S. Bock, and E. Vogel, Physica A **311**, 59 (2002).
[7] S. Bock, E. Bich, E. Vogel, A. S. Dickinson, and V. Vesovic, J. Chem. Phys. **117**, 2151 (2002).
[8] S. Bock, E. Bich, E. Vogel, A. S. Dickinson, and V. Vesovic, J. Chem. Phys. **120**, 7987 (2004).
[9] S. Bock, E. Bich, E. Vogel, A. S. Dickinson, and V. Vesovic, J. Chem. Phys. **121**, 4117 (2004).
[10] F. R. W. McCourt, V. Vesovic, W. A. Wakeham, A. S. Dickinson, and M. Mustafa, Mol. Phys. **72**, 1347 (1991).
[11] V. Vesovic, W. A. Wakeham, A. S. Dickinson, F. R. W. McCourt, and M. Thachuk, Mol. Phys. **84**, 553 (1995).
[12] C. F. Curtiss, J. Chem. Phys. **75**, 1341 (1981).
[13] A. S. Dickinson, R. Hellmann, E. Bich, and E. Vogel, Phys. Chem. Chem. Phys. **9**, 2836 (2007).
[14] R. Hellmann, E. Bich, and E. Vogel, J. Chem. Phys. **128**, 214303 (2008).
[15] L. Monchick and E. A. Mason, J. Chem. Phys. **35**, 1676 (1961).
[16] E. A. Mason and L. Monchick, J. Chem. Phys. **36**, 1622 (1962).
[17] G. A. Parker and R. T. Pack, J. Chem. Phys. **68**, 1585 (1978).
[18] J. Millat, V. Vesovic, and W. A. Wakeham, in *Transport Properties of Fluids: Their Correlation, Prediction and Estimation*, edited by J. Millat, J. H. Dymond, and C. A. Nieto de Castro (Cambridge University Press, Cambridge, UK, 1996), Chap. 4, pp. 29–65.
[19] E. L. Heck and A. S. Dickinson, Comput. Phys. Commun. **95**, 190 (1996).
[20] R. Hellmann, E. Bich, and A. S. Dickinson (unpublished).
[21] W. E. Köhler and G. W. 't Hooft, Z. Naturforsch. **34a**, 1255 (1979).
[22] G. C. Maitland, M. Rigby, E. B. Smith, and W. A. Wakeham, *Intermolecular Forces: Their Origin and Determination* (Clarendon, Oxford, 1987).
[23] J. Kestin, K. Knierim, E. A. Mason, B. Najafi, S. T. Ro, and M. Waldman, J. Phys. Chem. Ref. Data **13**, 229 (1984).
[24] J. H. Ferziger and H. G. Kaper, *The Mathematical Theory of Transport Processes in Gases* (North-Holland, Amsterdam, 1972).
[25] Y. Kagan and A. M. Afanasev, Sov. Phys. JETP **14**, 1096 (1962).
[26] L. A. Viehland, E. A. Mason, and S. I. Sandler, J. Chem. Phys. **68**, 5277 (1978).
[27] G. C. Maitland, M. Mustafa, and W. A. Wakeham, J. Chem. Soc., Faraday Trans. 2 **79**, 1425 (1983).
[28] E. L. Heck, A. S. Dickinson, and V. Vesovic, Chem. Phys. Lett. **240**, 151 (1995).
[29] L. J. F. Hermans, in *Status and Future Developments in the Study of Transport Properties*, NATO Advanced Studies Institute, Series C: Mathematical and Physical Sciences Vol. 361, edited by W. A. Wakeham, A. S. Dickinson, F. R. W. McCourt, and V. Vesovic (Kluwer, Dordrecht, 1992), pp. 155–174.
[30] J. Korving, H. Hulsman, H. F. P. Knaap, and J. J. M. Beenakker, Phys. Lett. **17**, 33 (1965).
[31] J. Korving, H. Hulsman, G. Scoles, H. F. P. Knaap, and J. J. M. Beenakker, Physica (Amsterdam) **36**, 177 (1967).
[32] H. Hulsman, E. J. van Waasdijk, A. L. J. Burgmans, H. F. P. Knaap, and J. J. M. Beenakker, Physica (Amsterdam) **50**, 53 (1970).
[33] J. Korving, Physica (Amsterdam) **50**, 27 (1970).
[34] H. Hulsman, F. G. van Kuik, K. W. Walstra, H. F. P. Knaap, and J. J. M. Beenakker, Physica (Amsterdam) **57**, 501 (1972).
[35] A. L. J. Burgmans, P. G. van Ditzhuyzen, H. F. P. Knaap, and J. J. M. Beenakker, Z. Naturforsch. **28a**, 835 (1973).
[36] E. L. Heck, A. S. Dickinson, and V. Vesovic, Mol. Phys. **83**, 907 (1994).
[37] V. Vesovic, S. Bock, E. Bich, E. Vogel, and A. S. Dickinson, Chem. Phys. Lett. **377**, 106 (2003).
[38] H. O'Hara and F. J. Smith, J. Comput. Phys. **5**, 328 (1970).
[39] See EPAPS Document No. E-JCPSA6-129-607830 for electronic files that contain these tables. For more information on EPAPS, see http://www.aip.org/pubservs/epaps.html
[40] R. A. Dawe, G. C. Maitland, M. Rigby, and E. B. Smith, Trans. Faraday Soc. **66**, 1955 (1970).
[41] E. Vogel, J. Wilhelm, C. Küchenmeister, and M. Jaeschke, High Temp. - High Press. **32**, 73 (2000).
[42] J. C. Rainwater and D. G. Friend, Phys. Rev. A **36**, 4062 (1987).
[43] E. Bich and E. Vogel, Int. J. Thermophys. **12**, 27 (1991).
[44] E. Vogel, C. Küchenmeister, E. Bich, and A. Laesecke, J. Phys. Chem. Ref. Data **27**, 947 (1998).
[45] P. Schley, M. Jaeschke, C. Küchenmeister, and E. Vogel, Int. J. Thermophys. **25**, 1623 (2004).
[46] C. Evers, H. W. Lösch, and W. Wagner, Int. J. Thermophys. **23**, 1411 (2002).
[47] E. F. May, R. F. Berg, and M. R. Moldover, Int. J. Thermophys. **28**, 1085 (2007).
[48] J. J. Hurly and J. B. Mehl, J. Res. Natl. Inst. Stand. Technol. **112**, 75 (2007).
[49] E. F. May, M. R. Moldover, R. F. Berg, and J. J. Hurly, Metrologia **43**, 247 (2006).
[50] R. F. Berg, Metrologia **42**, 11 (2005).
[51] R. F. Berg, Metrologia **43**, 183 (2006).
[52] E. Bich, R. Hellmann, and E. Vogel, Mol. Phys. **105**, 3035 (2007).
[53] J. Kestin and J. Yata, J. Chem. Phys. **49**, 4780 (1968).
[54] A. G. Clarke and E. B. Smith, J. Chem. Phys. **51**, 4156 (1969).
[55] J. Kestin, S. T. Ro, and W. A. Wakeham, Trans. Faraday Soc. **67**, 2308 (1971).
[56] J. M. Hellemans, J. Kestin, and S. T. Ro, Physica (Amsterdam) **65**, 376 (1973).
[57] G. C. Maitland and E. B. Smith, Trans. Faraday Soc. **70**, 1191 (1974).
[58] V. P. Slyusar, N. S. Rudenko, and V. M. Tretyakov, Fiz. Zhidk. Sostoyaniya **2**, 100 (1974).
[59] D. L. Timrot, M. A. Serednitskaya, and M. S. Bespalov, Dokl. Akad. Nauk SSSR **4**, 799 (1975).
[60] D. W. Gough, G. P. Matthews, and E. B. Smith, J. Chem. Soc., Faraday Trans. 1 **72**, 645 (1976).
[61] J. Kestin, H. E. Khalifa, and W. A. Wakeham, J. Chem. Phys. **67**, 4254 (1977).
[62] Y. Abe, J. Kestin, H. E. Khalifa, and W. A. Wakeham, Physica A **93**, 155 (1978).
[63] L. Zarkova, U. Hohm, and M. Damyanova, J. Phys. Chem. Ref. Data **35**, 1331 (2006).
[64] J. Kestin and W. Leidenfrost, Physica (Amsterdam) **25**, 1033 (1959).
[65] R. DiPippo, J. Kestin, and J. H. Whitelaw, Physica (Amsterdam) **32**, 2064 (1966).
[66] E. Bich, R. Hellmann, and E. Vogel, Mol. Phys. **106**, 813 (2008).
[67] E. B. Winn and E. P. Ney, Phys. Rev. **72**, 77 (1947).
[68] E. B. Winn, Phys. Rev. **80**, 1024 (1950).
[69] F. Hutchinson, J. Chem. Phys. **17**, 1081 (1949).

[70] R. Dawson, F. Khoury, and R. Kobayashi, AIChE J. **16**, 725 (1970).
[71] P. H. Oosting and N. J. Trappeniers, Physica (Amsterdam) **51**, 418 (1971).
[72] K. R. Harris, Physica A **94**, 448 (1978).
[73] C. J. Gerritsma and N. J. Trappeniers, Physica (Amsterdam) **51**, 365 (1971).
[74] A. S. Dickinson, Comput. Phys. Commun. **17**, 51 (1979).
[75] D. J. Kouri, in *Atom-Molecule Collision Theory: A Guide for the Experimentalist*, edited by R. B. Bernstein (Plenum, New York, 1979), Chap. 9, pp. 301–358.
[76] E. L. Heck, A. S. Dickinson, and V. Vesovic, Chem. Phys. Lett. **204**, 389 (1993).
[77] R. Hellmann, E. Bich, E. Vogel, A. S. Dickinson, and V. Vesovic (unpublished).
[78] F. A. Gianturco, M. Venanzi, and A. S. Dickinson, J. Chem. Phys. **93**, 5552 (1990).